Spatiotemporal processing of whisker input supports texture discrimination by a brain-based device

Anil K. Seth, Jeffrey L. McKinstry, Gerald M. Edelman, and Jeffrey L. Krichmar
The Neurosciences Institute, 10640 John Jay Hopkins Drive, San Diego, CA 92121, USA
seth@nsi.edu, mckinstry@nsi.edu, edelman@nsi.edu, krichmar@nsi.edu

Abstract

Sensory signals from whiskers are typically rich in both spatial and temporal structure, and are used by many animals to guide a variety of adaptive behaviors. To explore possible neural mechanisms underlying whisker-guided behavior, we constructed Darwin IX, a mobile physical device equipped with artificial whiskers and a neural simulation based on the rat somatosensory (whisker) system. We show that neuronal units with time-lagged response properties, together with the selective modulation of neural connection strengths, provide a plausible neural mechanism for the spatiotemporal transformations of sensory input necessary for both texture discrimination and selective conditioning to textures.

1. Introduction

Haptic sensory signals provided by vibrissae (whiskers) guide a variety of adaptive behaviors in many animals. For example, rodents use their whiskers to discriminate among different textures and to learn associations between specific textures and aversive or appetitive events (Carvell and Simons, 1990, Harvey et al., 2001, Prigg et al., 2002). Whisker signals typically have rich spatial and temporal structure as a consequence of interactions among the spatial arrangement of whiskers on the rat face, the spatial properties of the object being whisked, and the movement over time of the whiskers past the object; this movement can be generated by active sweeping of whiskers across object surfaces as well as by locomotion of the animal. Spatiotemporal processing is therefore fundamental to the neural operations underlying whisker-guided behavior.

The whisker system of the rat has been studied extensively as a model for spatiotemporal sensory processing (Moore et al., 1999, Ghazanfar and Nicolelis, 2001, Ahissar and Arieli, 2001). For example, neurons in layer V of primary somatosensory cortex (S1) have been shown to possess spatiotemporally defined receptive fields, i.e. individual neurons respond best to different whiskers as a function of post-stimulus time (Ghazanfar and Nicolelis, 1999). However, since most studies of the rat whisker system involve anesthetized or head-fixed animals, and many of these involve manipulating single whiskers, relatively little is known about the spatiotemporal operations of the complete system during natural whisker-guided behavior.

For example, the neural mechanisms underlying texture discrimination by the rat remain poorly understood. One possibility is that surface texture is encoded by intrinsic vibrational modes of the whiskers, so that different textures elicit different spectral profiles (Mehta and Kleinfeld, 2004). While this mechanism may be mechanically plausible (Fend et al., 2003), evidence is lacking for corresponding neural operations in the behaving rat. A second possibility, consistent with observations of spatiotemporal receptive fields, is that texture is encoded by patterns of convergent activity across multiple whiskers. However, direct neurobiological support for such a mechanism is again absent.

Experimental assessment of these possibilities requires specific hypotheses that incorporate neuronal mechanisms, phenotypes, and behavioral interactions with the environment. To test the idea that texture discrimination can be supported by convergent inputs from multiple whiskers, we constructed Darwin IX. Darwin IX is a mobile physical device equipped with artificial whiskers and a simulated nervous system incorporating neuroanatomical and neurophysiological features of the rat somatosensory (whisker) system, as well as neural areas involved in fear conditioning and learning. We investigate the hypothesis that neuronal units that respond to whisker input with unit-specific time delays (Saul and Humphrey, 1992), together with the selective modulation of neural connections strengths, provide a plausible neural mechanism for the spatiotemporal transformations of sensory input needed for both texture discrimination and selective conditioning to textures.

Darwin IX is the latest in a series of 'brain-based devices' (BBDs) that have been constructed over the last 12 years (Edelman et al., 1992, Almassy et al., 1998, Krichmar and Edelman, 2002, Seth et al., in press). All BBDs in the Darwin series have the following attributes: 1) An embodied morphology that allows for active exploration

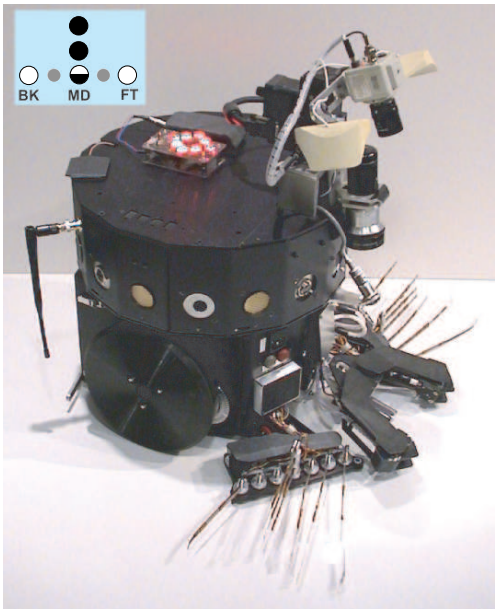

Figure 1: Darwin IX consists of a mobile base (Nomadic Technologies Inc.) equipped with several sensors and effectors including left and right whisker arrays, and a neural simulation running on a remote cluster of computer workstations. The arrangement of a whisker array is shown in the inset. Each array has 7 whiskers arranged in a row of 5 and a column of 3. Whiskers used for wall following are marked in white (BK,MD,FT). Whiskers that provide input to the neural simulation are marked in black. Note that one whisker (white/black) is used for both purposes. Whiskers marked in gray (small circles) are not used in the present model.

in a real-world environment, including sensors such as cameras, microphones, proximity sensors, and artificial whiskers. 2) A neural simulation to control the BBD's behavior, incorporating detailed neuroanatomy and neurophysiology based on vertebrate nervous systems. 3) A value system that signals the salience of environmental cues and that modulates plasticity in the nervous system resulting in modification of the device's behavior. A key feature of all BBDs is that they allow neuronal responses to be followed in detail at all levels of control, while the device is behaving. Such detailed correlations of behavioral and brain responses, which would not be possible in animal experiments, can provide insights into and form the basis for predictions regarding the neuronal basis of adaptive behavior.

In our experiments with Darwin IX, the device autonomously explored a walled environment containing two distinct textures each consisting of patterns of pegs embedded in the walls. It became conditioned to avoid one of the textures by association of this texture with an innately aversive simulated 'foot-shock'. Darwin IX demonstrated its conditioned behavior by freezing and then moving away from walls containing the texture corresponding to the aversive sources.

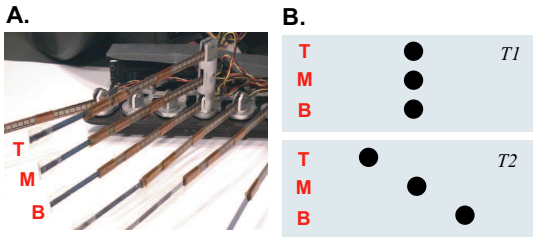

Figure 2: **A.** Detail of a whisker array: The top (T), middle (M), and bottom (B) whiskers in the column are labeled; these whiskers provide input to the neural simulation. **B.** Schematic of textures $T1$ and $T2$. Each texture consists of pegs embedded in a wall; pegs are aligned in rows corresponding to the whiskers in a column. Pegs in the top row deflect the top whisker (T), and similarly for pegs in the middle row (M) and the bottom row (B).

2. Methods

Darwin IX consists of a mobile robotic base containing infra-red (IR) proximity sensors, custom-built whisker arrays (Fig. 1), and a cluster of workstations that run the simulated nervous system and control the device's behavior. The cluster consists of six 1.4 GHz Pentium IV workstations running Message Passing Interface (MPI) parallel software under the Linux operating system. One workstation receives whisker and IR input information, and transmits motor commands, via a wireless modem. A microcontroller (PIC17C756A) onboard the base samples input and status from the sensors and controls RS-232 communication between the robotic base and the workstations.

A simulation cycle of Darwin IX consists of the following events: Sensory input is processed, the state of the neural simulation is updated, and motor output is generated. In our experiments, execution of each simulation cycle requires approximately 100ms of real time.

2.1 Artificial whisker design

Each whisker array consists of seven whiskers arranged in a column of three and a row of five (see Fig. 1, inset, and Fig. 2A). Whisker columns supply input to the simulated nervous system, while whiskers in the rows support innate avoidance and wall following behaviors (see *2.2. Innate behavior*). Each whisker consists of two 4cm by 0.63cm polyamide strips, adhered back-to-back, that are responsive to bend (Abrams/Gentile Entertainment). These strips are typically used as strain sensors in devices such as virtual reality gloves. Each strip has 20 resistive areas embedded regularly along its length, providing a resistance of $\sim$10KΩ when the strip is unbent and $\sim$50KΩ when the strip is maximally bent. Each strip

detects bending in only one direction, hence the back-to-back arrangement. Voltage signals from each pair of strips (i.e. a whisker) are converted to a single signal ranging from 0V (maximum deflection in one direction) to 5V (maximum deflection in the opposite direction). These voltages are converted into digital signals, ranging from 0 to 255, by a 12-bit analog-to-digital converter at a sample rate of 40Hz.

During each simulation cycle of Darwin IX a 'packet' of 4 signals from each whisker is received by the neural simulation. For whisker w_k at simulation cycle t, the corresponding packet is $[w_{k1}(t), w_{k2}(t), w_{k3}(t), w_{k4}(t)]$, where $w_{k4}(t)$ is the most recent. The first signal in each packet, $w_{k1}(t)$, which we call the 'current whisker value', is used for guiding Darwin IX's wall following behavior; all four signals provide input to the neural simulation (see *2.4. Whisker input and lag cells*).

2.2 Innate behavior

Darwin IX is equipped with innate behavioral responses. The default behavior of Darwin IX is to move forward in a straight line at a speed of ∼8cm/sec. If Darwin IX approaches a wall head-on to within a distance of ∼4cm, an avoidance response is triggered by either of two IR sensors, one facing front-left, and the other facing front-right: The device stops, backs up (∼10cm), and then turns $\sim\pi/6$ away from the wall before resuming it's default behavior.

Darwin IX has an innate freezing/escape response which is triggered by a simulated 'foot-shock'. A downward-facing IR sensor at the front of the device detects reflective construction paper ('foot-shock pads') on the floor of the arena; activation of this sensor evokes neural activity in area M_{ave} (see 2.3. *Neuroanatomy*) which triggers the behavioral response. This response consists of continued movement for ∼5.5s, freezing for ∼4s, then a turn away from the wall by an angle randomly chosen from the interval $[\pi/4, 3\pi/4]$.

Darwin IX also has an innate wall following capability such that, on encountering a wall, the device moves parallel to the wall at a distance suitable for the detection of embedded textures (see Fig. 2B). Wall following is based on signals from the backmost (BK), the 'middle' whisker, which is lowest of the vertical stack (MD), and the frontmost (FT) on each side (see Fig. 1, inset). For each of these whiskers, a running average of the current whisker value ($\overline{w}$) is maintained over 75 simulation cycles. This average is updated at every cycle except when the current whisker value differs by more than 10 from the corresponding average (signifying whisker deflection; recall that the range of the current whisker value is 0-255). For each whisker k on each side, a 'deflection' value wd is calculated as:

$$wd_k(t) = |w_{k1}(t) - \overline{w}_k(t)| \quad (1)$$

Side	Whisker	φ_w	$g_w(wd(t) > 0)$	$g_w(wd(t) \leq 0)$
Left	BK	89	0.05	0.075
	MD	33	0.1	0.2
Right	BK	110	0.075	0.15
	MD	28	0.15	0.30

Table 1: Wall following by Darwin IX. Scaling factors g_w and φ_w were calibrated according to the physical response characteristics of each whisker, in order to allow Darwin IX to follow walls at a distance appropriate for the detection of textures. Factor g_w varies according to the direction of the corresponding whisker deflection such that there is a bias in favor of turning towards a wall.

Wall following of a left(right) wall is triggered when any deflection value for the left(right) whiskers exceeds 15. During each cycle of wall following, adjustments are made to the speed of the wheel furthest from the wall (the contralateral wheel); the other (ipsilateral) wheel remains at the default speed of $W_{def} = 35$. Contralateral wheel speeds are set using:

$$W_{speed} = W_{def} - back - mid - front \quad (2)$$

where $front = 0.25(wd_{FT})$, $mid = g_w(wd_{MD} - \varphi_w)$, and $back = g_w(wd_{BK} - \varphi_w)$, and where mid and $back$ are bounded in the range ± 5, and g_w (a scaling factor) and φ_w (a threshold) were calibrated for each whisker according the physical response characteristics of the whiskers (see Table 1). Additionally, g_w varies according to the sign of the corresponding wd such that there is a bias in favor of turning towards a wall (see Table 1, columns 4 and 5).

2.3 Neuroanatomy

Darwin IX's simulated nervous system contains areas analogous to the somatosensory pathway in the rat brain, specifically the (ventromedial) nuclei of the thalamus, and primary and secondary somatosensory areas (in our model, $Th \rightarrow S1 \rightarrow S2$), as well as neural areas involved in fear conditioning and learning.

Areas $S1$ and Th are subdivided into left (L) and right (R) regions and further into 'top' (T), 'middle' (M) and 'bottom' (B) subregions, such that each subregion receives input from a single whisker in the column on the corresponding side. These subregions are analogous to so-called whisker 'barrels' (in rat S1) and 'barreloids' (in rat thalamus); as in Darwin IX, each whisker barrel/barreloid in the rat contains cells that respond preferentially to a specific whisker (Woolsey and Van der Loos, 1970).

A global diagram of Darwin IX's simulated nervous system is given in Fig. 3. It comprises 17 areas, 1101 neuronal units (see Table 2), and ∼8400 synaptic connections (see Table 3). Neuronal units in area Th respond

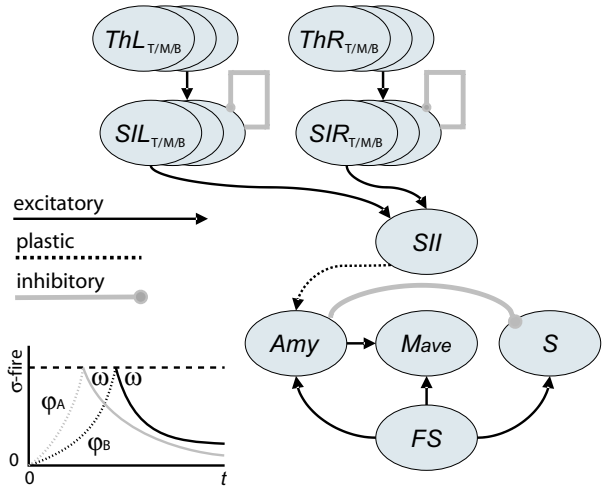

Figure 3: Global neuroanatomy of Darwin IX. See text for details. **Inset**. The operation of two idealized lag cells (A and B). The post-stimulus internal state of cell A (s_A^{in}) rises quickly (gray dashed line), at a rate determined by φ_A. The internal state of B (s_B^{in}) rises more slowly (black dashed line, φ_B). When the internal state of each cell reaches a threshold (σ^{fire}), output is generated (solid lines) which decays at a rate determined by ω.

Area	Size	σ^{fire}	ω	g
$Th(6)$	1x20	0.3	0.8	-
$S1(6)$	1x20	0.1	0.0	1.0
$S2$	30x30	0.2	0.8	1.0
S	1x1	-0.10	0.0	1.0
Amy	1x1	0.0	0.0	1.75
M_{ave}	3x6	0.0	0.0	1.0
FS	1x1	-	-	-

Table 2: Neuronal unit parameters for Darwin IX. Area Th consists of 6 separate 'barreloid areas' which take input directly from the 3 whiskers in each column on each side of Darwin IX. Activity in area FS is triggered by detection of 'foot-shock' pads by Darwin IX's downward-facing IR sensor. Size indicates the number of neuronal units in each area or sub-area. Neuronal units in each area apart from area FS have a specific firing threshold (σ^{fire}), a persistence parameter (ω) and a scaling factor (g).

to whisker input with unit-specific time delays (see *2.4. Whisker input and lag cells*). These units project topographically to the corresponding units of $S1$. Each barrel in $S1$ has local inhibitory connections which serve to increase the activity contrast among neuronal units. All barrels in $S1$ project to area $S2$ such that each neuronal unit in $S2$ takes input from 3 neuronal units, each of which is in a different barrel of either the left sub-area or the right sub-area of $S1$. This arrangement ensures that synaptic input to a neuronal unit in $S2$ is sparse and balanced. A deflection of a particular sequence of Darwin IX's whiskers leads to a spatiotemporal pattern of activity in $S2$. Such a dynamic sequence is comparable to that observed in the rat brain (Ghazanfar and Nicolelis, 1999).

Darwin IX's nervous system also contains areas supporting the acquisition of conditioned aversion (see *2.7. Aversive conditioning*). Area FS is activated by detection of a 'foot-shock' (see *2.8. Experimental environment and protocol*), and projects to areas *Amy*, M_{ave} and S. Area *Amy* is analogous to the amygdala, a neural area which has been widely implicated in the acquisition of conditioned fear (Maren and Fanselow, 1996). Area M_{ave} is analogous to a motor area, activity in which elicits an innate aversive freezing/escape response.

Activity in the simulated value system, area S, signals the occurrence of salient sensory events and this activity contributes to the modulation of plastic connection strengths in the pathway $S2 \rightarrow Amy$. Initially, S is activated by detection of simulated 'foot-shock'. Activity in S is analogous to that of ascending neuromodulatory systems in that it is triggered by salient events, influences large regions of the simulated nervous system (see *2.6. Synaptic plasticity*), and persists for several cycles (Schultz et al., 1997). After conditioning, S is activated by patterns of activity in $S2$ corresponding to the aversive texture (see *2.7. Aversive conditioning* and *2.8. Experimental environment and protocol*).

2.4 Whisker input and lag cells

Whisker input to the neural simulation is provided by transforming each whisker packet into a vector of 'difference values' according to:

$$\begin{aligned} diff_k = [&w_{k4}(t) - w_{k3}(t), w_{k3}(t) - w_{k2}(t), \\ &w_{k2}(t) - w_{k1}(t), w_{k1}(t) - w_{k4}(t-1)] \end{aligned} \quad (3)$$

for whisker w_k at simulation cycle t. These values from the whisker in each column provide input to the corresponding barreloids of area Th.

Each barreloid of area Th contains 20 'lag' cells; neuronal units which respond to input with cell-specific time delays (cells with similar properties have been found in the visual thalamus of the cat, see Saul and Humphrey, 1992). Each lag cell is characterized by an internal state (s_i^{in}), an output (s_i), and a cell-specific lag parameter set to be $\psi_i = \frac{0.2}{i}$, $i \in \{1, 2 \ldots 20\}$ for cell i in each barreloid. When triggered by a whisker deflection, the internal state s_i^{in} of cell i in the corresponding subregion increases at rate determined by the lag parameter ψ_i. When this internal state reaches a threshold, the cell begins to emit an output signal and s_i^{in} is reset to zero.

Because of differences in ψ_i among lag cells, cells in a barreloid fire with a range of delays, from 1 to 20 simulation cycles, following deflection of the corresponding whisker (see Fig. 3, inset).

Specifically, s_i^{in} in the barreloid corresponding to whisker w_k, is updated according to:

$$s_{ki}^{in}(t{+}1) = \begin{cases} 0.2 & s_{ki}^{in}(t) < 0.2, \overline{diff}_k(t) > 3.0 \\ 0 & s_{ki}^{in}(t) \geq \sigma_i^{fire} \\ (1+\psi_i)(s_{ki}^{in}(t)) & \text{otherwise} \end{cases} \quad (4)$$

where $\overline{diff}_k(t)$ is the average $diff_k(t)$ value (a value exceeding exceeding 3.0 signifies a whisker deflection), and σ_i^{fire} is a unit-specific firing threshold (Table 2).

The output s_{ki} is calculated using

$$s_{ki}(t+1) = \begin{cases} \tanh(10(\omega_i(s_{ki}(t)))) & s_{ki}^{in}(t) < \sigma_i^{fire} \\ \tanh(10(\omega_i(s_{ki}(t)) & \\ \quad +(1-\omega_i)s_{ki}^{in}(t))) & \text{otherwise} \end{cases} \quad (5)$$

where ω_i determines the persistence of unit activity from one cycle to the next (Table 2). This value is fed as input into neuronal units in the corresponding barrel of area $S1$.

2.5 Neuronal dynamics

With the exception of the lag cells in area Th, the state of each neuronal unit in Darwin IX is determined by a mean firing rate variable s, which corresponds to the average activity of a group of roughly 100 real neurons over 100ms (s_{ki} of a lag cell is equivalent to the mean firing rate of neuronal units in other areas).

The mean firing rate (s) of each neuronal unit ranges from 0 (quiescent) to 1 (maximal firing). For all neuronal units, except those in areas Th and FS, the total input to unit i is given by

$$A_i(t) = \sum_{l=1}^{M} \sum_{j=1}^{Nl} c_{ij} s_j(t) \quad (6)$$

where M is the number of different anatomically defined connection types and Nl is the number of connections per type M projecting to unit i (see Table 3). The mean firing rate of unit i is given by

$$s_i(t+1) = \phi(\tanh(g_i(A_i(t) + \omega s_i(t)))) \quad (7)$$

where $\phi(x) = 0$ for $x < \sigma_i^{fire}$, otherwise $\phi(x) = x$, g_i is a scale factor, and ω determines the persistence of unit activity (Table 2).

Projection	Arbor	P	$c_{ij}(0)$
$Th \rightarrow S1$	[]0x0	1.0	13.0,15.0
$S1 \rightarrow S1(intra)$	[]2x8	1.0	-0.45,-0.6
$S1 \rightarrow S2$	special	-	0.25,0.25
$FS \rightarrow Amy$	non-topo	1.0	5.0,5.0
$Amy \rightarrow M_{ave}$	non-topo	1.0	40.0,40.0
$FS \rightarrow M_{ave}$	non-topo	1.0	50.0,50.0
$FS \rightarrow S$	non-topo	1.0	50.0,50.0
$Amy \rightarrow S$	non-topo	1.0	-50.0,-50.0
$S2 \rightarrow Amy$	non-topo	1.0	0.0001,0.0003

Table 3: Properties of anatomical projections in Darwin IX. Neuronal units connect with a probability (P) and projection shape (Arbor) which can be rectangular "[]" with a height and width (h x w), non-topographical "non-topo" where all pairs of neuronal units have an equal probability of being connected, or 'special' (see text). The initial connection strengths, $c_{ij}(0)$, are set randomly within the range (min, max). Connections marked with "intra" denote those within a sub-area.

2.6 Synaptic plasticity

Synaptic plasticity in Darwin IX acts to strengthen connections between simultaneously active neuronal units in areas $S2$ and Amy. This process is 'value dependent', i.e. the degree of change is modulated by activity in the simulated value system (area S) according to the following rule:

$$\Delta c_{ij}(t+1) = \eta s_j(t) BCM(s_i(t))(V(t) - 0.1) \quad (8)$$

where η is a fixed learning rate ($\eta = 1.4$), $s_i(t)$ and $s_j(t)$ are the activities of the post- and pre-synaptic units respectively and $V(t)$ is the mean activity in area S. The term $(V(t)-0.1)$ causes depression of plastic connections in the absence of value system activity.

The function $BCM()$ is based on the rule of Bienenstock et al. (1982) and is implemented as follows ($\rho = 6$, $\theta_1 = \theta_2 = 0.1$, $k1 = k2 = 0.45$):

$$BCM(x) = \begin{cases} 0 & x < \theta_1 \\ k_1(\theta_1 - x) & \theta_1 \leq \frac{\theta_1+\theta_2}{2} \\ k_1(x - \theta_2) & \frac{\theta_1+\theta_2}{2} \leq x < \theta_2 \\ \frac{k_2 \tanh(\rho(x-\theta_2))}{\rho} & \text{otherwise} \end{cases} \quad (9)$$

2.7 Aversive conditioning

Synaptic plasticity supports conditioned aversion to texture as follows. Area S maintains a baseline level of activity (0.1) in the absence of input ($\sigma_i^{fire} = -0.1$, see Table 2). Detection of a simulated foot-shock (see *2.8. Experimental environment and protocol*) causes neuronal units in area FS to produce a steady output of magnitude 1.0. This output pushes activity in area S above

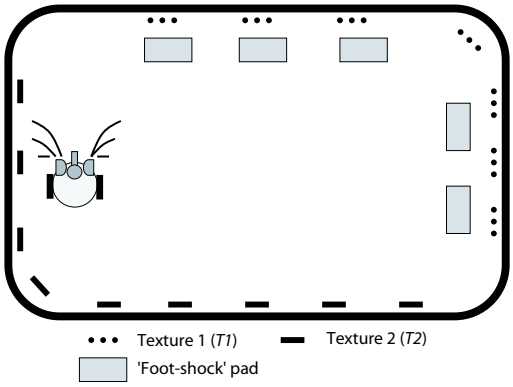

Figure 4: Experimental setup for Darwin IX. Darwin IX explored a walled enclosure (2.41m x 2.95m) with textures $T1$ and $T2$ on the walls. Instances of each texture were regularly spaced along the walls at intervals of ∼30cm. Located on the floor adjacent to $T1$ patterns were 'foot-shock' pads made of reflective construction paper. Training and testing was repeated for each Darwin IX subject after exchanging the positions of $T1$ and $T2$.

baseline, which causes potentiation of synapses onto neuronal units in area *Amy* from units in $S2$ corresponding to the currently present texture (see equations (8,9)). Freezing/escape responses are triggered by activity in M_{ave} exceeding a threshold (0.5) as a result of input from areas FS and/or *Amy* (see Fig. 3). This model also supports extinction of conditioned responses: If *Amy* is activated without any corresponding foot-shock, area S will be inhibited such that its firing rate will drop below baseline, and currently active synapses between $S2$ and *Amy* will be weakened (see equations (8,9)).

2.8 Experimental environment and protocol

Fig. 4 shows the overall arrangement of Darwin IX's environment. One texture ($T1$) consists of a vertically aligned column of pegs, the other ($T2$) consists of a vertically staggered set of pegs with offsets of ∼6cm (see Fig. 2B). Two adjacent walls contained $T1$, the other two contained $T2$, and either $T1$ or $T2$ can be associated with a simulated aversive foot-shock. Note that Darwin IX typically travels in both clockwise and anticlockwise directions around the environment such that the textures deflect both the left and right whisker arrays. Moreover, in the case of $T2$, the pattern of whisker deflection depends on the direction of travel.

Experiments were divided into training and testing stages. During training, either $T1$ or $T2$ was paired with foot-shock and Darwin IX autonomously explored its enclosure for 25,000 simulation cycles, corresponding to ∼48 encounters with each wall and ∼24 aversive responses to the simulated foot-shock. During testing, the foot-shock pads were removed and Darwin IX was allowed to explore its enclosure for 15,000 simulation cycles. Training and testing were repeated using three different Darwin IX "subjects" initialized with different random seeds, and pairing both $T1$ and $T2$ with foot-shocks (six training/testing episodes in total). During training and testing of each subject, responses of all neuronal units were recorded and saved for analysis. The position of Darwin IX was also continuously recorded by an overhead camera that detected an array of LEDs positioned on the top surface of the robotic device, the images from which were time-stamped for analysis.

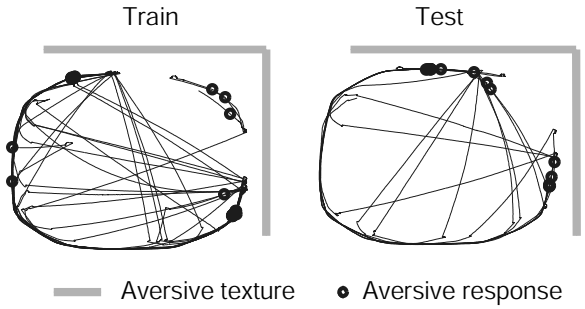

Figure 5: Conditioned aversion to textures by Darwin IX. The line tracings show the trajectory of a single Darwin IX subject during aversive conditioning to texture $T1$ (left), and during testing (right). Large black dots show locations of aversive responses, gray shading shows locations of $T1$. During testing all freezing/escape responses occurred in proximity to the aversive texture $T1$.

3. Results

3.1 Selective conditioning to textures

Texture discrimination by Darwin IX subjects was assessed by monitoring trajectories during testing. Fig. 5 shows the behavior of a single Darwin IX subject during training in which foot-shock (the unconditioned stimulus, or UCS) was paired with $T1$ (the conditioned stimulus, or CS), and during testing, in which the foot-shock pads were removed. Most aversive responses, both unconditioned (UR, in response to the UCS), and conditioned (CR, in response to the CS), occurred in regions associated with the aversive texture. This response pattern is similar to that observed during conditioning of animals to aversive stimuli (Mackintosh, 1983).[1]

Taking into account data from all subjects reveals near perfect conditioned avoidance of aversive textures. During testing, Darwin IX subjects which were trained to avoid $T1$ made CRs on 96.6% (S.E. = 0.18%) of encounters with $T1$. When trained to avoid $T2$, these subjects made CRs on 97.9% (S.E. = 0.14%) of encounters with $T2$ during testing. Only 3.2% of all aversive responses

[1]Short movies showing Darwin IX's behavior during encounters with neutral and aversive textures can be viewed at `www.nsi.edu/nomad/whisker/movies/`.

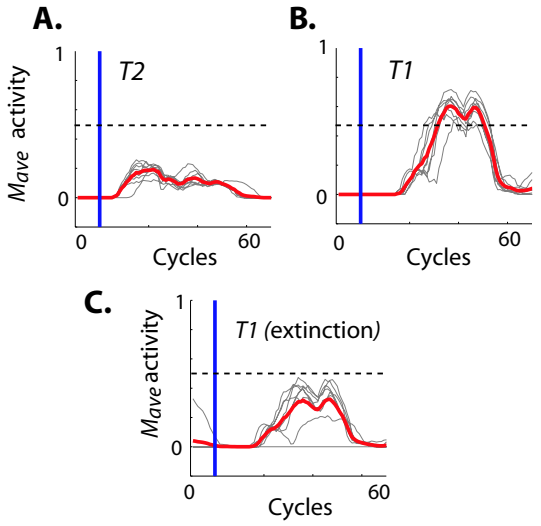

Figure 6: Neural activity in area M_{ave} during testing. Each panel shows mean M_{ave} activity over 60 time-steps for 10 encounters by the left whisker array with textures *T2* (A) or *T1* (B). The vertical line indicates the moment of deflection of the first whisker during each encounter, the thick line shows the grand mean M_{ave} response, and the dashed line shows the threshold for production of an aversive response. Panels A and B show encounters from early in testing (up to 10,000 time-steps). Panel C shows encounters from late in testing (after 20,000 time-steps).

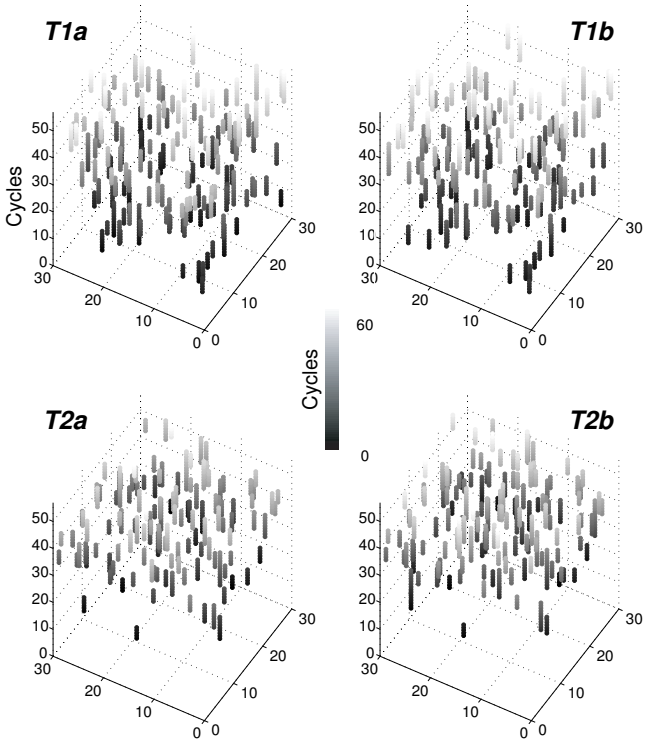

Figure 7: Spatiotemporal response properties of neuronal units in $S2$. The top panels show $S2$ activity during two separate encounters (a,b) with texture $T1$ by Darwin IX's left whisker column. The bottom panels show encounters of the same whiskers with texture $T2$. Each panel shows the activity of the 30x30 matrix of $S2$ neuronal units (x and y axes) over 60 post-stimulus cycles (indicated by the z axis as well as by the gray scale). Neuronal units are shown if their activity exceeded a threshold (0.25).

during testing occurred inappropriately, i.e. in response to whisker deflections by walls or by the texture not associated with foot-shock.

Fig. 6 illustrates the motor neuronal responses associated with the expression of conditioned aversion. Each panel shows mean activity in area M_{ave} from several encounters by the left whisker array with both neutral (*T2*) and aversive (*T1*, the CS) textures during testing. Fig. 6A shows that M_{ave} responses to the neutral texture ($T2$) are reliably weak, and hence do not trigger aversive responses. By contrast, M_{ave} responses to the CS ($T1$) are reliably strong (Fig. 6B) and do trigger aversive responses.

3.2 Extinction

Similar to behavioral data for aversive conditioning in animals (Mackintosh, 1983), Darwin IX's conditioned responses to aversive textures are subject to extinction. During testing, early encounters with the aversive textures evoke aversive responses. They also — as a result of inhibitory projections from *Amy* to S — suppress activity in the value system (area S). Inhibition of S activity below baseline leads to synaptic depression of active projections between $S2$ and *Amy*, and hence extinction of the conditioned response to the corresponding texture (see equations (8,9)). Note that during training, the inhibitory projections from *Amy* to S are counteracted by the excitatory projections from area FS to S.

The neural events underlying extinction in Darwin IX are illustrated in Fig. 6C, which shows M_{ave} responses late in testing (after ∼20,000 time-steps). Peak M_{ave} responses to the CS have diminished below the threshold at which motor aversive responses are triggered.

3.3 Spatiotemporal neural activity

Darwin IX's ability to categorize textural stimuli is supported by spatiotemporal patterns of activity in neural area $S2$. Each texture deflects whiskers in a column in a specific temporal order. The lag cells in area Th and neural units downstream in $S1$ (see Fig. 3) present a pattern of activity with both a spatial component (i.e. the particular whisker) and a temporal component (i.e. the time since deflection). $S2$ responds to particular combinations of this $S1$ activity.

The population response of $S2$ to a texture was specific and repeatable. Fig. 7 shows representative $S2$

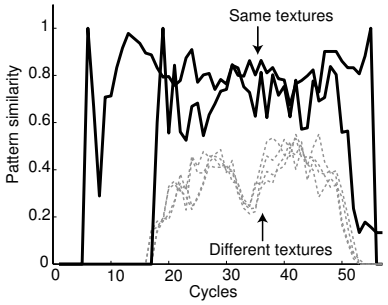

Figure 8: Similarity over time between pairwise combinations of activity patterns shown in Fig. 7, calculated as $sim(i,j) = v_i(t) \bullet v_j(t)$ where $v_i(t)$ is the normalized neuronal unit activity vector for pattern i at time t. Patterns representing the same texture are highly similar over time (solid lines; $sim(T1a, T1b)$, $sim(T2a, T2b)$), but patterns representing different textures are not similar (dashed lines; $sim(T1a, T2a)$, $sim(T1a, T2b)$, $sim(T2a, T1a)$, $sim(T2a, T1b)$).

activity patterns during testing of a Darwin IX subject. The top panels show $S2$ activity during encounters of the left whisker column with texture $T1$. The bottom panels show encounters of the same whiskers with texture $T2$. While all panels show complex spatiotemporal patterns of activity, the top panels are highly similar to each other, the bottom panels are also highly similar to each other, but the top and bottom panels are dissimilar. This observation is supported quantitatively by measures of pattern similarity over time for all possible pairs, calculated as the normalized vector product (see Fig. 8). As shown in this figure, there is high similarity between activity patterns representing the same texture, but not between activity patterns representing different textures.

4. Discussion

Darwin IX demonstrates the ability to categorize objects based on haptic data and to learn behavioral responses selective to specific textures. Observations of Darwin IX show that time-lagged neuronal responses to somatosensory input together with value-dependent synaptic plasticity provide a plausible mechanism for the spatiotemporal transformations of sensory input needed for texture discrimination. Darwin IX also shows that this mechanism can provide a basis for selective conditioned aversion to textures.

A key feature of Darwin IX is the incorporation of artificial whiskers that provide signals according to the degree of bend. Although the material properties of our artificial whiskers are clearly different those of rat whiskers, the rat somatosensory system appears capable of extracting similar signals. Szwed and colleagues have recently found neurons in the lower brainstem of the rat which are sensitive to pressure against objects, where pressure would correspond to degree of whisker bend (Szwed et al., 2003). Of course, rat whiskers may signal along many more dimensions than we capture in our design. For example, the intrinsic vibrational modes of whiskers may be significant for texture discrimination.

Distinguishing among textures using only the information provided by whiskers involves multiple spatiotemporal transformations. In our experiments, Darwin IX's self-generated movement transforms the spatial patterns of textures into temporal patterns of whisker deflections. These patterns are themselves transformed into spatiotemporal patterns of neural activity in area $S2$, via a combination of the intrinsic properties of lag cells in area Th and the arrangement of projections in the pathway $Th \rightarrow S1 \rightarrow S2$. As a result, neuronal units in $S2$ respond to specific combinations of whisker deflections with particular post-stimulus delays. Analysis of neural activity in $S2$ revealed the formation of spatiotemporal activity patterns corresponding to specific haptic perceptual categories (Fig. 7).

These observations are consistent with certain empirical data obtained from the rat. For example, Shuler and colleagues have shown that under bilateral whisker stimulation, the responses of rat S1 neurons to ipsilateral stimulation depended on both the spatial location and the relative timing of the bilateral stimuli (Shuler et al., 2001). Also, Ghazanfar and Nicolelis have identified cells in layer V of rat S1 that have spatiotemporal receptive fields, that is, individual neurons respond best to different whiskers as a function of post-stimulus time (Ghazanfar and Nicolelis, 1999). The spatiotemporal patterns of activity observed in area $S2$ of our model have similar properties: The sensitivity of a neuronal unit in $S2$ to a whisker deflection will vary over time as a function of the temporal pattern of preceding whisker deflections.

What neural circuitry might account for these sorts of spatiotemporal response properties? Our model shows the plausibility of a mechanism based on the convergence of inputs from different sources, each with different temporal dynamics. Empirical studies suggest that such circuits may exist in brains. For example, two classes of neurons — 'lagged' and 'non-lagged' — have been identified in the visual thalamus of the cat (Saul and Humphrey, 1992).

In the rat somatosensory system, the situation is less clear. While no direct equivalent to the 'lag' cells of our model have yet been identified, neurons have been found with latencies that vary as a function of input frequency during single whisker stimulation in restrained rats (Ahissar and Arieli, 2001). Also, neurons have been found which have specific latencies with respect to the onset of a whisking cycle during active whisking (Szwed et al., 2003). Both types of neuron may

participate in convergent input mechanisms that transform temporal patterns into spatial patterns. Alternatively, Ghazanfar and Nicolelis (2001) suggest that the spatiotemporal properties of rat S1 neurons may depend on the convergence of asynchronous inputs from different brainstem nuclei, together with feedback from cortex. The resolution of these issues remains a challenge for neuroscientists.

A second question, which also remains open, is whether these spatiotemporal activity patterns are used to support texture discrimination. Our model shows that they can be, and it makes the prediction that disruption of the spatiotemporal patterning of activity in rat S1 should impair its ability to distinguish among textures. However, alternative mechanisms for texture discrimination can be envisaged. For example, texture may be encoded in terms of the intrinsic vibrational modes of whiskers (Mehta and Kleinfeld, 2004). In support of this idea, Fend and colleagues have shown that plucked rat whiskers appear to have a limited number of vibration frequencies, the relative amplitudes of which are modulated in specific ways by different grades of sandpaper (Fend et al., 2003). Of course, these mechanisms are not mutually exclusive and it is possible that the rat brain uses multiple pathways to achieve ethologically significant discriminations.

As well as a simulated somatosensory system, Darwin IX incorporates neural areas analogous to areas involved in fear conditioning and learning, and, as a result, reproduces several features of these phenomena.

Texture discrimination by Darwin IX was assessed behaviorally by a paradigm in which one texture (the CS) was paired with a simulated foot-shock (the UCS). In this paradigm, simulated foot-shock triggers a freezing/avoidance response (the unconditioned response, or UR) and activates a value system which modulates synaptic plasticity between $S2$ and Amy. Activity in Amy due to the CS evokes the same avoidance response (now called the conditioned response, or CR) via excitatory projections to M_{ave}. Repeated pairings of the CS and the US therefore result in a transference of the UCS-UR association to the CS (and CR). By these means, Darwin IX acquired a conditioned aversion to specific textures similar to that shown by animals in comparable situations (see Figs. 5 and 6) (Mackintosh, 1983, Harvey et al., 2001, Prigg et al., 2002).

Also consistent with animal studies (Mackintosh, 1983) is the extinction to conditioned aversion displayed by Darwin IX. During testing, repeated encounters with the CS in the absence of the US caused suppression of activity in the value system (area S) and a corresponding depression of active synapses between $S2$ and Amy. After many such encounters, the activity in Amy evoked by the CS became insufficient to drive M_{ave} above the threshold needed to evoke an avoidance response (Fig. 6).

Central to these behaviors is area Amy, which is analogous to the rodent amygdala. The amygdala has long been implicated in fear conditioning (Kluver and Bucy, 1937), and recent evidence has pointed to roles in the association of sensory information as well as in the execution of motor programs (Maren and Fanselow, 1996). Area Amy in the present model also sustains this dual role, taking input from area $S2$ as well as area FS, and projecting to M_{ave}.

The role of synaptic plasticity in the amygdala during fear conditioning remains a focus of research. Our model suggests a mechanism of plasticity between the amygdala and neurons carrying information about the CS (in our model, area $S2$). Consistent with this idea, synaptic potentiation in the amygdala has been induced *in vivo* by stimulation of afferent connections in putative CS pathways (Maren and Fanselow, 1995). However, establishing a direct link between such potentiation and learned behavior remains a challenge. Our model also suggests that CR extinction may involve synaptic depression in the same pathways that mediate acquisition; again, this hypothesis awaits experimental investigation.

Brain-based devices are not only useful for testing theories of the brain, they also provide a foundation for the development of intelligent machines that follow neurobiological rather than computational principles in their construction. Darwin IX extends previous BBDs in the series by incorporating a sense of touch, which allows texture discrimination and navigation in the dark.

Whisker-based systems have been the subject of increasing attention among engineers interested in building adaptive machines. However, previous work on whisker-based perception in robots has focused on texture discrimination or contact localization by fixed whiskers (Russell, 1992, Kaneko et al., 1998, Fend et al., 2003), or on obstacle avoidance by a mobile robot (Brooks, 1989, Jung and Zelinsky, 1996). Darwin IX extends these studies by showing texture discrimination using whisker arrays mounted on a behaving device, and by incorporating a neural simulation based on the rat somatosensory system.

5. Conclusion

Spatiotemporal transformations are fundamental to neural operations underlying adaptive behavior. Nowhere is this more evident than in the somatosensory system of the rat. Darwin IX illustrates a neural mechanism, based on the rat somatosensory system, which is capable of orchestrating spatiotemporal transformations of whisker signals to allow texture discrimination, and selective conditioning to textures, in a real world environment. Future developments in the Darwin series will explore the integration of somatosensory perception with other modalities, for example vision (Seth et al., in

press), and other behavioral tasks, for example navigation.

Acknowledgment

This work was supported by the W.M. Keck Foundation and the Neurosciences Research Foundation. We thank Jim Snook, Donald Hutson, and Doug Moore for their contribution to the design of Darwin IX. We are also grateful to our anonymous reviewers for useful feeback.

Address correspondence to Anil K. Seth (*seth@nsi.edu*).

References

Ahissar, E. and Arieli, A. (2001). Figuring space by time. *Neuron*, 32:185–201.

Almassy, N., Edelman, G., and Sporns, O. (1998). Behavioral constraints in the development of neuronal properties: a cortical model embedded in a real-world device. *Cerebral Cortex*, 8:346–361.

Bienenstock, E., Cooper, L., and Munro, P. (1982). Theory for the development of neuron selectivity: orientation specificit and binocular interaction in the visual cortex. *Journal of Neuroscience*, 2(1):32–48.

Brooks, R. (1989). A robot that walks: Emergent behaviors from a carefully evolved network. *Neural Computation*, 1:153–162.

Carvell, G. and Simons, D. (1990). Biometric analyses of vibrissal tactile discrimination in the rat. *Journal of Neuroscience*, 10(8):2638–48.

Edelman, G., Reeke, G., Gall, W., Tononi, G., Williams, D., and Sporns, O. (1992). Synthetic neural modeling applied to a real-world artifact. *Proc. Nat. Acad. Sci. USA*, 89(15):7267–71.

Fend, M., Bovet, S., Yokoi, H., and Pfeifer, R. (2003). An active artificial whisker array for texture discrimination. In *Proceedings of the IEEE/RSJ International Conference on Intelligent Robots and Systems (IROS)*.

Ghazanfar, A. and Nicolelis, M. (1999). Spatiotemporal properties of layer V neurons of the rat primary somatosensory cortex. *Cerebral Cortex*, 9:348–361.

Ghazanfar, A. and Nicolelis, M. (2001). The structure and function of dynamic cortical and thalamic receptive fields. *Cerebral Cortex*, 11:183–193.

Harvey, M., Bermejo, R., and Zeigler, H. (2001). Discriminative whisking in the head-fixed rat: optoelectronic monitoring during tactile detection and discrimination tasks. *Somatosens. Mot. Res.*, 18(3):211–22.

Jung, D. and Zelinsky, A. (1996). Whisker-based mobile robot navigation. In *Proceedings of the IEEE/RSJ International Conference on Intelligent Robots and Systems (IROS)*, pages 497–504.

Kaneko, M., Kanayama, N., and Tsuji, T. (1998). Active antenna for contact sensing. *IEEE Transactions on Robotics and Automation*, 14(2):278–291.

Kluver, H. and Bucy, P. (1937). An analysis of certain effects of bilateral temporal lobectomy in the rhesus monkey, with special reference to 'psychic blindness'. *American Journal of Physiology*, 119:352–353.

Krichmar, J. and Edelman, G. (2002). Machine psychology: Autonomous behavior, perceptual categorization and conditioning in a brain-based device. *Cerebral Cortex*, 12(8):818–30.

Mackintosh, N. (1983). *Conditioning and associative learning*. Oxford University Press, Oxford.

Maren, S. and Fanselow, M. (1995). Synaptic plasticity in the basolateral amygdala induced by hippocampal stimulation in vivo. *Journal of Neuroscience*, 15:7548–7564.

Maren, S. and Fanselow, M. (1996). The amygdala and fear conditioning: has the nut been cracked? *Neuron*, 16(2):237–40.

Mehta, S. and Kleinfeld, D. (2004). Frisking the whiskers: Patterned sensory input in the rat vibrissa system. *Neuron*, 41:181–184.

Moore, C., Nelson, S., and Sur, M. (1999). Dynamics of neuronal processing in rat somatosensory cortex. *Trends in Neuroscience*, 22:513–520.

Prigg, T., Goldreich, D., Carvell, G., and Simons, D. (2002). Texture discrimination and unit recordings in the rat whisker/barrel system. *Physiol. Behav.*, 77.

Russell, R. (1992). Using tactile whiskers to measure surface contours. In *Proc. IEEE International Conference on Robotics and Automation*, pages 1295–1300.

Saul, A. and Humphrey, A. (1992). Evidence of input from lagged cells in the lateral geniculate nucleus to simple cells in cortical area 17 of the cat. *J. Neurophysiol.*, 68(4):1190–208.

Schultz, W., Dayan, P., and Montague, P. (1997). A neural substrate of prediction and reward. *Science*, 275(5306):1593–9.

Seth, A., McKinstry, J., Edelman, G., and Krichmar, J. (in press). Visual binding through reentrant connectivity and dynamic synchronization in a brain-based device. *Cerebral Cortex*.

Shuler, M., Krupa, D., and Nicolelis, M. (2001). Bilateral integration of whisker information in the primary somatosensory cortex of rats. *Journal of Neuroscience*, 21(14):5251–5261.

Szwed, M., Bagdasarian, K., and Ahissar, E. (2003). Encoding of vibrissal active touch. *Neuron*, 40:621–630.

Woolsey, T. and Van der Loos, H. (1970). The structural organization of layer IV in the somatosensory region SI of mouse cerebral cortex. The description of a cortical field composed of discrete cytoarchitectonic units. *Brain Research*, 17(2):205–42.